Supporting Information for "Frictional origin of slip events of the Whillans Ice Stream, Antarctica"

Gauthier Guerin[1], Aurélien Mordret[2,3], Diane Rivet[1], Bradley P. Lipovsky[4]&

Brent M. Minchew[3]

[1]Université Côte dAzur, CNRS, Observatoire de la Côte dAzur, IRD, Géoazur, Sophia Antipolis, 06560 Valbonne, France

[2]Université Grenoble Alpes, Univ. Savoie Mont Blanc, CNRS, IRD, IFSTTAR, ISTerre, UMR 5275, 38000 Grenoble, France.

[3]Department of Earth, Atmospheric and Planetary Sciences, Massachusetts Institute of Technology (MIT), Cambridge, Massachusetts, USA.

[4]Department of Earth and Planetary Sciences, Harvard University, Cambridge, MA, USA.

Contents of this file

Introduction

S1. Rupture velocity from the GPS data.

For each of the 78 stick-slip events analyzed, we pick at each GPS station the time for which the ice velocity exceeds 10 m/d. We interpolate the travel time measured at each station onto a regular grid using a spline-in-tension scheme, to obtain a smooth and continuous travel time surface. We then compute the spatial gradient of the travel time surface and take the inverse of the gradient's magnitude to obtain a map of the rupture front velocity for each event. The final map is an average of the 78 rupture velocity maps (Fig. 1c).

S2. Computation and stack of the correlations.

The seismic data come from the network 2C (see Acknowledgements section) and were downloaded and their instrument response corrected using the obspyDMT software (Hosseini & Sigloch, 2017). The first step of data processing consists of cross-correlating the data from the 33 seismic stations and stacking the cross-correlations adequately. We use the MSNoise package to perform the computation (Lecocq et al., 2014). The raw data are whitened between 0.01 Hz and 9.5 Hz, clipped for amplitudes above 1.5 root-mean-square of each trace. The resulting correlations are further filtered between 0.05 Hz and 9 Hz. We compute all four components of the correlation tensor containing Rayleigh waves (vertical-vertical, radial-radial, vertical-radial, and radial-vertical).

To increase the signal-to-noise ratio (SNR) by an order of magnitude, we stack the correlations accordingly to the timing of each stick-slip event, a scheme inspired by the approach of Hillers et al. (2015). We retrieve the start time of all stick-slip events from the GPS data, and we focus on an 8h-long window centered on the onset of the 78 stick-slip

cycles. We stack over 78 cycles the correlations which have the same relative time with respect to the origin time of each event (Fig. S1). The effective duration of the data used for one correlation therefore increases to 13 hours. In this 8-hour long window, we are left with 96 correlations per station pair for the whole duration of the analysis.

S3. dc/c measurements and mapping.

We follow the approach of Brenguier et al. (2014) to invert a dc/c time series for each pair of stations. This method requires measuring the relative velocity variations between every 10-minute long correlation among the 96 correlations for one station pair. Two parameters regularize the least square inversion: α, the smoothing strength, and β, the temporal covariance length. We chose α=5000 and β=2.

Before measuring dc/c for a station pair, we apply a Wiener filter on the 96 correlations (Moreau et al., 2017) to enhance the SNR and stabilize the measurements. The velocity changes are measured with the moving window cross-spectral (MWCS) analysis between 0.2 and 0.5 Hz. We perform the measurements on both the causal and acausal sides of the correlations, in a 50 s long window starting at the time corresponding to a 1 km/s propagation velocity. The Rayleigh wave phase velocity in the ice being 1.6 km/s, we ensure that the waves in the coda windows are scattered waves. We used an MWCS moving window of 7.5 s, with 3 s steps, and we set the quality criterion to keep a measurement as 0.7 for the minimum coherency and 0.2 s for the maximum error. This error is used to remove very large outliers: it corresponds roughly to a dc/c value of 0.5% for propagation distances around 30 km, much larger than what would be expected from velocity changes

in the till layer. We measure the dc/c for the four correlation components containing Rayleigh waves and we average the four time series for each station pair.

Since we measure dc/c in the early coda, we can consider that the spatial sensitivity of the velocity changes is the highest around the stations (Hobiger et al., 2012; Obermann et al., 2013; Brenguier et al., 2014). For a given station, we can localize the velocity changes by averaging all dc/c time series in which this station is involved and associate the dc/c value to the position of the station. The final dc/c maps are obtained by natural-neighbor interpolation (Sibson & Barnett, 1981) of the localized dc/c.

S4. Period of oscillation of an ice plate

The period of oscillation of the fundamental mode of a free standing square thin plate is given by (Jones, 1975):

$$T_0 = 1.09\sqrt{\rho_i \frac{a^4}{Eh^2}} = 73min, \tag{1}$$

with $\rho_i = 920kg/m^3$ the density of ice, $a = 100km$ the size of the plate, $h = 800m$, the thickness of the plate and $E = 9GPa$ the Young's modulus of the ice.

S5. Poroelastic changes from *dc/c*.

We use an effective medium model (Dvorkin et al., 1999; Leeman et al., 2016) to relate the shear wave velocity of a saturated porous medium to the effective pressure and porosity. Following, the shear wave velocity V_s is defined as (Gassmann, 1951):

$$V_s = \sqrt{\frac{G_{sat}}{\rho_b}}, \tag{2}$$

where G_{sat} is the saturated shear modulus and $\rho_b = (1-\phi)\rho_{mat} + \phi\rho_w$ is the bulk density of the medium which depends on the porosity ϕ, the density of the rock matrix ρ_{mat} and the water density $\rho_w = 1.0 g/cm^3$.

Since the shear modulus of pore water is zero and all the shear strength is carried by the solid frame, we have $G_{sat} = G_{dry}$ (Gassmann, 1951), where G_{dry} is the effective shear modulus of the solid matrix and is defined for an arbitrary porosity ϕ lower than a critical porosity $\phi_c = 0.4$ (Dvorkin et al., 1999):

$$G_{dry}(\phi) = \left(\frac{\phi/\phi_c}{G_{HM} + Z} + \frac{1 - \phi/\phi_c}{G + Z} \right)^{-1} - Z \,, \tag{3}$$

with

$$Z = \frac{G_{HM}}{6} \left(\frac{9K_{HM} + 8G_{HM}}{K_{HM} + 2G_{HM}} \right) . \tag{4}$$

The critical porosity is the porosity at which the medium becomes a fluid suspension with solid grains that are not in contact anymore and cannot transfer load. It is the transition porosity between a frame-supported medium to a fluid-supported medium (Nur et al., 1998). At zero porosity, the bulk and shear modulus of the matrix are K and G, respectively, and ν is its Poisson ratio. At the critical porosity ϕ_c, the effective bulk and shear moduli of the dry matrix are (Dvorkin et al., 1999):

$$G_{HM}(P_e) = \frac{5 - 4\nu}{5(2-\nu)} \left(\frac{3n^2(1-\phi_c)^2 G^2}{2\pi^2(1-\nu)^2} P_e \right)^{1/3} , \tag{5}$$

with

$$K_{HM}(P_e) = \left(\frac{n^2(1-\phi_c)^2 G^2}{18\pi^2(1-\nu)^2} P_e \right)^{1/3} ; \tag{6}$$

where P_e is the effective pressure and $n = 8.0$ is the average number of contacts per grain in the sphere pack. The matrix shear modulus at zero porosity is taken as the Hill's average of the shear moduli of the mineral constituents of the till:

$$G = \frac{1}{2}\left[\sum w_i G_i + \left(\sum \frac{w_i}{G_i}\right)^{-1}\right] ; \tag{7}$$

where w_i is the volumetric fraction of the i-th constituent of the till (Table S1). The matrix density ρ_{mat} and its Poisson ratio ν are also taken as the Hill's averages of the mineral constituents of the till.

S6. Relative change of till shear wave from dc/c.

To compute the depth sensitivity of Rayleigh waves at different periods, we use a velocity model (Luthra et al., 2016) discretized every meter and made of three layers: 700 m of ice (V_s = 1860 m/s), 10 m of till (V_s = 350 m/s) and a bedrock half-space (V_s = 2600 m/s). The sensitivity $\partial c/\partial V_s$ of the Rayleigh phase velocity c to change in shear wave velocity V_s, for the considered period band and averaged over the ten meters of till is approximately $\partial c/\partial V_s = 0.03$ (Fig. S2). We can, therefore, estimate the relative change of V_s in the till as

$$\frac{dV_s}{V_s} = \frac{dc}{c}\frac{\partial V_s}{\partial c}\frac{c}{V_s} = -0.05\% \times \frac{1}{0.03} \times \frac{1600}{350} = -7.6\% , \tag{8}$$

which gives, for a Rayleigh phase velocity in the ice c = 1600 m/s, till shear-wave velocity V_s = 350 m/s and dc/c = -0.05%, dV_s/V_s = -7.6%.

S7. Velocity changes due to volumetric deformation of the ice

The shear-wave velocity β is a function of the shear modulus μ and the density ρ:

$$\beta = \sqrt{\frac{\mu}{\rho}}. \tag{9}$$

If the medium experiences a variation in its elastic properties we obtain the following equation:

$$\frac{\delta\beta}{\beta} = \frac{1}{2}\left[\frac{\delta\mu}{\mu} - \frac{\delta\rho}{\rho}\right]. \tag{10}$$

The dilation is the relative change in an elementary volume and can be related in a linear elastic medium to a change in density and a change in pressure:

$$\xi = \frac{\delta V}{V} = -\frac{\delta\rho}{\rho} = -\frac{\delta P}{K}, \tag{11}$$

where ξ is the dilation, P the pressure, V the volume and K the bulk modulus. A change in pressure is thus function of the dilation:

$$\delta P = -K\xi. \tag{12}$$

The relation between shear modulus and pressure perturbations assuming a constant temperature in the medium and a linear elastic behavior is the following:

$$\frac{\delta\mu}{\mu} = \frac{\partial\mu}{\partial P}\frac{\delta P}{\mu}. \tag{13}$$

We finally express the relative velocity change as a function of dilation, and the shear modulus using eqs. 10, 12 and 13 :

$$\frac{\delta\beta}{\beta} = \frac{\xi}{2}\left[1 - \frac{\partial\mu}{\partial P}\frac{K}{\mu}\right], \tag{14}$$

or using the relations of the bulk and shear moduli with the Poisson's ratio ν:

$$\frac{\delta\beta}{\beta} = \frac{\xi}{2}\left[1 - \frac{2(1+\nu)}{3(1-2\nu)}\frac{\partial\mu}{\partial P}\right]. \tag{15}$$

Taking ice Poisson's ratio around 0.33 and weak sensitivity of ice shear modulus to pressure changes at small pressures ($\mid \partial\mu/\partial P \mid \ll 1$; Shaw (1986)), we obtain

$$\left|\frac{\delta\beta}{\beta}\right| \approx \mid \xi \mid . \tag{16}$$

This derivation does not take into account potential changes in ice porosity during the cycle, that could be translated into shear-wave velocity changes. If a porosity change occurs during the stick-slip event due to the ice deformation, one can expect the change to be maximum when the deformation is maximum. However, we observe that the seismic velocity keeps decreasing even after the end of the slip. This indicates that the velocity changes cannot be entirely due to ice elastic deformation effects.

References

Brenguier, F., Campillo, M., Takeda, T., Aoki, Y., Shapiro, N., Briand, X., ... Miyake, H. (2014). Mapping pressurized volcanic fluids from induced crustal seismic velocity drops. *Science*, *345*(6192), 80–82.

Dvorkin, J., Prasad, M., Sakai, A., & Lavoie, D. (1999). Elasticity of marine sediments: Rock physics modeling. *Geophysical research letters*, *26*(12), 1781–1784.

Gassmann, F. (1951). Elasticity of porous media. *Vierteljahrsschrder Naturforschenden Gesselschaft*, *96*, 1–23.

Hillers, G., Retailleau, L., Campillo, M., Inbal, A., Ampuero, J.-P., & Nishimura, T. (2015). In situ observations of velocity changes in response to tidal deformation from analysis of the high-frequency ambient wavefield. *Journal of Geophysical Research: Solid Earth*, *120*(1), 210–225.

Hobiger, M., Wegler, U., Shiomi, K., & Nakahara, H. (2012). Coseismic and postseismic elastic wave velocity variations caused by the 2008 Iwate-Miyagi Nairiku earthquake, Japan. *Journal of Geophysical Research: Solid Earth*, *117*(B9).

Hosseini, K., & Sigloch, K. (2017). ObspyDMT: a Python toolbox for retrieving and processing large seismological data sets. *Solid Earth*(5), 1047–1070.

Jones, R. (1975). An approximate expression for the fundamental frequency of vibration of elastic plates. *Journal of Sound and Vibration*, *38*(4), 503–504.

Lecocq, T., Caudron, C., & Brenguier, F. (2014). MSNoise, a python package for monitoring seismic velocity changes using ambient seismic noise. *Seismological Research Letters*, *85*(3), 715–726.

Leeman, J., Valdez, R., Alley, R., Anandakrishnan, S., & Saffer, D. (2016). Mechanical and hydrologic properties of Whillans Ice Stream till: Implications for basal strength and stick-slip failure. *Journal of Geophysical Research: Earth Surface*, *121*(7), 1295–1309.

Luthra, T., Anandakrishnan, S., Winberry, J.-P., Alley, R. B., & Holschuh, N. (2016). Basal characteristics of the main sticky spot on the ice plain of Whillans Ice Stream, Antarctica. *Earth and Planetary Science Letters*, *440*, 12–19.

Moreau, L., Stehly, L., Boué, P., Lu, Y., Larose, E., & Campillo, M. (2017). Improving ambient noise correlation functions with an SVD-based Wiener filter. *Geophysical Journal International*, *211*(1), 418–426.

Nur, A., Mavko, G., Dvorkin, J., & Galmudi, D. (1998). Critical porosity: A key to relating physical properties to porosity in rocks. *The Leading Edge*, *17*(3), 357–362.

Obermann, A., Planes, T., Larose, E., Sens-Schönfelder, C., & Campillo, M. (2013). Depth sensitivity of seismic coda waves to velocity perturbations in an elastic heterogeneous medium. *Geophysical Journal International*, *194*(1), 372–382.

Shaw, G. H. (1986). Elastic properties and equation of state of high pressure ice. *The Journal of chemical physics*, *84*(10), 5862–5868.

Sibson, R., & Barnett, V. (1981). Interpreting multivariate data. *A brief description of natural neighbor interpolation*, 21–36.

Minerals	Clay	Quartz	Feldspar
Ratio	0.5049	0.2373	0.2578
Shear modulus (GPa)	20	47	38
Bulk modulus (GPa)	42.5	37.7	70
Density (g/cm^3)	2.626	2.65	2.56

Table S1. Till composition (Leeman et al., 2016)

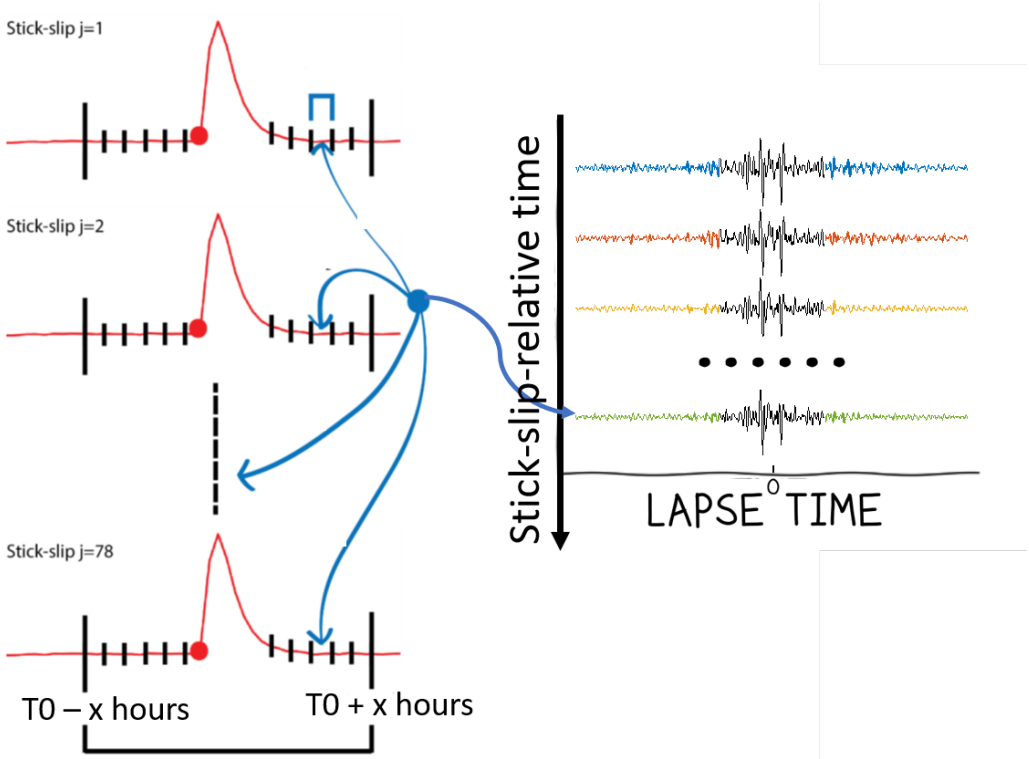

Figure S1. Correlation stacking scheme. The seismic data (in black) are sorted, centered and cut according to the starting time T0 of each stick-slip event observed on the GPS time-series (in red). Each 10 minute-long seismic data segment with the same relative starting time is correlated for each pair of seismic stations. Then, these correlations are stacked for each stick-slip event. Therefore, each pair of seismic stations results in 96 correlations sorted along the stick-slip relative time.

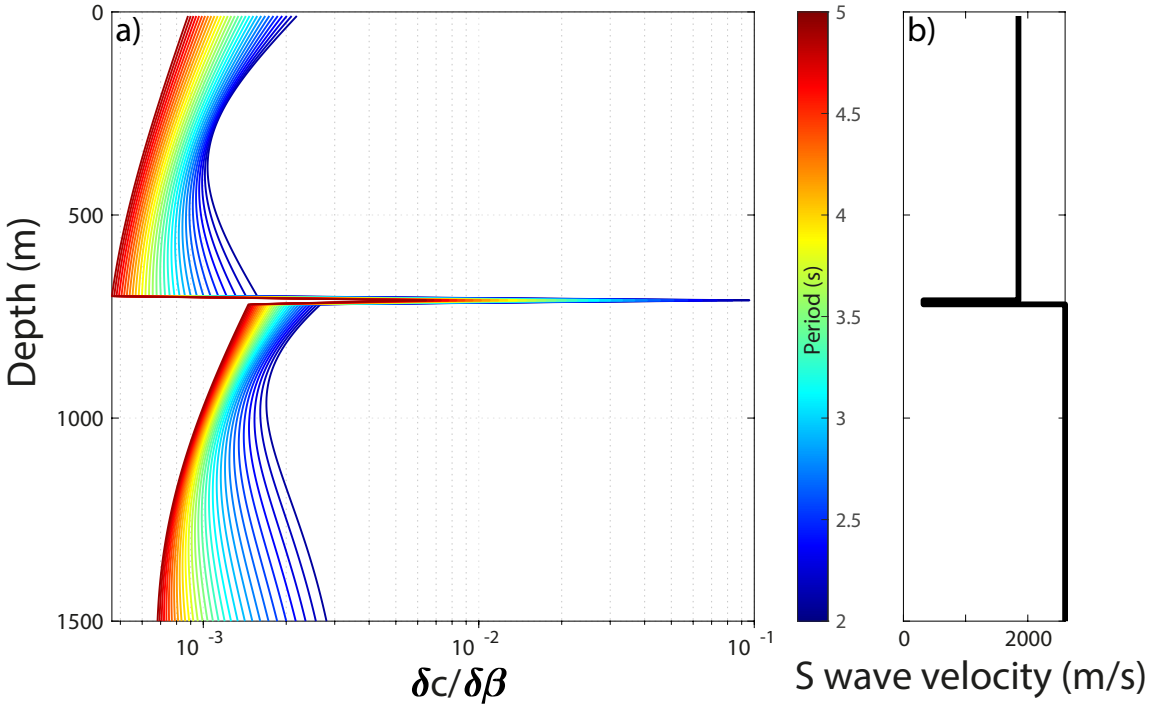

Figure S2. a) Rayleigh wave sensitivity kernels at periods between 2 and 5 s for the velocity model shown in b), taken from Luthra et al. (2016). $\delta c/\delta\beta$ is the sensitivity of shear-wave velocity β to a change in phase velocity c.

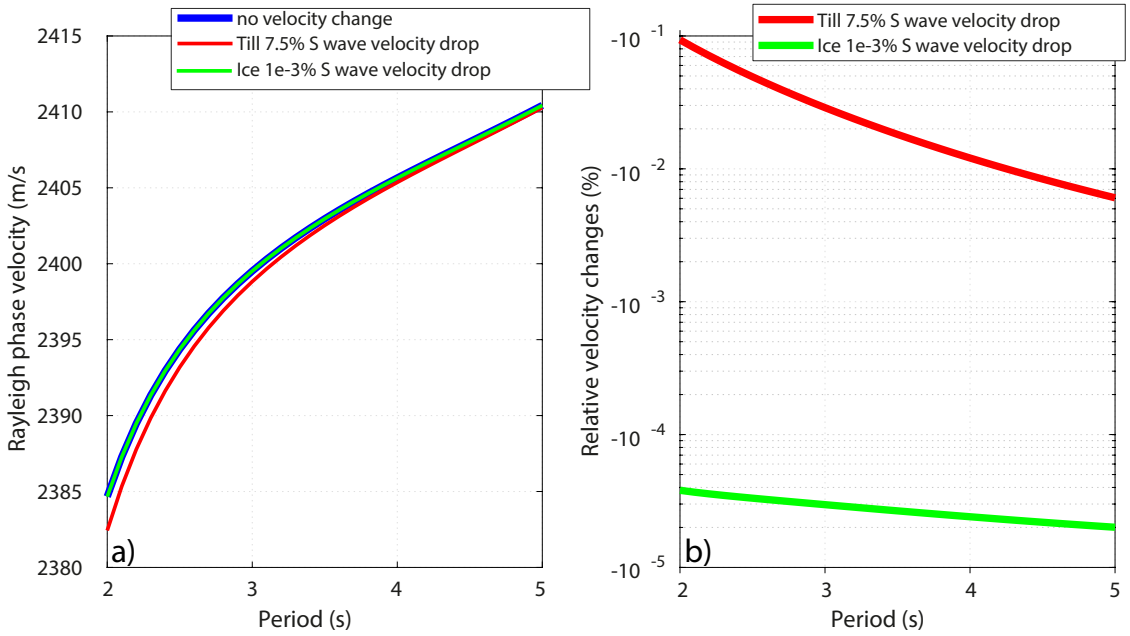

Figure S3. Effect of 0.001% velocity change in the 700 m thick ice column (green curves) compared to 7.5% velocity change in the 10 m thick till layer (red curves), in absolute phase velocities (a) and relative phase velocity changes (b).